Proc. Natl. Acad. Sci. USA
Vol. 95, pp. 13042–13047, October 1998
Developmental Biology

Detection of targeted *GFP-Hox* gene fusions during mouse embryogenesis

(gene targeting/*Hoxa1*/*Hoxc13*)

ALAN R. GODWIN*, H. SCOTT STADLER*, KOTOKA NAKAMURA†, AND MARIO R. CAPECCHI‡

Howard Hughes Medical Institute, Department of Human Genetics, University of Utah School of Medicine, Salt Lake City, UT 84112

Contributed by Mario R. Capecchi, September 3, 1998

ABSTRACT **The ability to use a vital cell marker to study mouse embryogenesis will open new avenues of experimental research. Recently, the use of transgenic mice, containing multiple copies of the jellyfish gene encoding the green fluorescent protein (GFP), has begun to realize this potential. Here, we show that the fluorescent signals produced by single-copy, targeted *GFP* in-frame fusions with two different murine *Hox* genes, *Hoxa1* and *Hoxc13*, are readily detectable by using confocal microscopy. Since *Hoxa1* is expressed early and *Hoxc13* is expressed late in mouse embryogenesis, this study shows that single-copy *GFP* gene fusions can be used through most of mouse embryogenesis. Previously, targeted *lac*Z gene fusions have been very useful for analyzing mouse mutants. Use of *GFP* gene fusions extends the benefits of targeted *lac*Z gene fusions by providing the additional utility of a vital marker. Our analysis of the *Hoxc13*^{GFPneo} embryos reveals GFP expression in each of the sites expected from analysis of *Hoxc13*^{lacZneo} embryos. Similarly, *Hoxa1*^{GFPneo} expression was detected in all of the sites predicted from RNA *in situ* analysis. GFP expression in the foregut pocket of *Hoxa1*^{GFPneo} embryos suggests a role for *Hoxa1* in foregut-mediated differentiation of the cardiogenic mesoderm.**

The jellyfish, *Aequorea victoria*, produces a protein, green fluorescent protein (GFP), which absorbs blue light and emits green light. In the years since the cDNA encoding this protein was cloned (1), it has become an important reporter gene in both prokaryotic and eukaryotic organisms. In contrast to β-galactosidase (β-gal) detection protocols, no exogenous substrates are required, only molecular oxygen and excitation light being needed to reveal the active chromophore (2). Therefore, *GFP* fusion genes can be detected in living organisms as they develop. In addition, GFP is small (26.9 kDa) and functions as a monomer, making it ideal for protein fusions (3), whereas the widely used reporter β-gal is much larger (135 kDa) and functions as a tetramer (4–5).

Use of *GFP* reporter genes in mammalian systems has been facilitated by the generation of derivatives optimized for mammalian codon usage. These alterations, which aid translational efficiency, may improve protein folding as well. In addition, several amino acid changes that shift the excitation spectrum toward red and increase fluorescent signal strength have been incorporated (6–7). To date, the use of optimized GFP variants in vertebrates have been limited to transgenic mice (8–10) and zebrafish (11–15) and to cell-labeling studies in *Xenopus* (16) and mouse (17) embryos. The mammalian studies have involved either injection of large numbers of plasmids encoding GFP or production of transgenic animals containing multiple-copy tandem arrays of the gene to obtain strong fluorescent signals. Notably, it has been possible to generate mice that express GFP in all cells (8). This strain can be used similarly to the *lac*Z-expressing Rosa26 mice in chimeric studies, with the additional advantage that individual chimeras can be examined over time (18–19). Importantly, ubiquitous expression of high levels of GFP appears to be nontoxic (8). In addition, it has been recently demonstrated that GFP can be used as a cell lineage marker in living mouse embryos (17). Although these GFP-expressing mice provide significant advances in the use of a vital marker for developmental studies, the aforementioned applications are subject to all the limitations inherent in transgenic methodology. For example, signal strength has varied widely among different transgenic lines (13); position effects may influence the ability to completely recapitulate all aspects of normal temporal and spatial regulation of gene expression, and transgenes are often subject to silencing.

Here, we demonstrate that GFP is detectable when a single-copy of the gene is targeted into two separate *Hox* genes. In addition, we show that single-copy *GFP* fusion gene expression can be examined both early in mammalian embryogenesis when the embryo is relatively clear and in organ preparations late in embryogenesis when the embryo is opaque. These targeted *GFP*-gene fusions provide the same benefits as targeted *lac*Z fusions (20) including retention of all cis-acting elements, lack of position effects, and labeling of the mutant cells in homozygotes but in addition, include the advantages of a vital marker. In particular, optical sectioning of GFP-expressing embryos by laser scanning confocal microscopy enables careful three-dimensional analysis of gene expression patterns without histological sectioning.

MATERIALS AND METHODS

Vector Construction. The *GFP* fusion-gene cassette was constructed starting with the *Nco*I–*Afl*II fragment containing the *GFP*-coding region from pEGFP (CLONTECH). This fragment was resected with S_1 nuclease up to the first base of the second codon and cloned into a derivative of pSP72 (Promega). In addition, the *Not*I site between the *GFP*-coding region and Poly(A) addition signal was removed. Finally, an MC1neo cassette (21) flanked by *lox*P sites was cloned into the vector. The final vector allows the entire *GFP lox*P *neo lox*P cassette to be excised by using *Kpn*I, *Sal*I, or *Bam*HI.

The *Hoxa1* insertion vector was constructed from a 7.8-kb *Cla*I fragment containing the *Hoxa1*-coding region. The *GFP*

Abbreviations: GFP, green fluorescent protein; E, embryonic day; ES cell, embryonic stem cell; *Hox*, homeobox containing; HSV, herpes simplex virus; β-gal, β-galactosidase.

*A.R.G. and H.S.S. contributed equally to this manuscript.

†Present address: Department of Biological Chemistry, University of California, Los Angeles, CA 90095.

‡To whom reprint requests should be addressed at: Howard Hughes Medical Institute, University of Utah, 15 North 2030 East, Suite 5400, Salt Lake City, UT 84112-5331. e-mail: mario.capecchi@genetics.utah.edu.

The publication costs of this article were defrayed in part by page charge payment. This article must therefore be hereby marked "*advertisement*" in accordance with 18 U.S.C. §1734 solely to indicate this fact.

*lox*P *neo* cassette was ligated into a unique *Aat*II site present in exon 2. Verification of the correct reading frame across the *Hoxa1/GFP* junction was determined by manual dideoxy sequencing (United States Biochemical). Finally, the herpes simplex virus (HSV) thymidine kinase gene (TK1) (22) was inserted 5′ of the *Hoxa1* sequences.

The *Hoxc13* insertion vector was constructed by inserting the *GFP* fusion gene cassette into a previously described bacteriophage lambda clone (23), which carries an *Xho*I linker insertion at the *Bst*EII site in the third helix of the homeodomain of *Hoxc13*, generating an in-frame fusion of the *Hoxc13*- and *GFP*-coding regions. The resulting fusion gene is directly analogous to the previously described *Hoxc13*^{lacZneo} allele (23).

Generation of Targeted Cell Lines and Germline Transmitting Mice. Targeting vectors were electroporated into R1 embryonic stem (ES) cells (24) and subjected to positive–negative selection as described (22). Targeted disruptions for each gene were detected by Southern transfer analyses. Targeted colonies were microinjected into C57BL/6J blastocysts to generate chimeric mice as previously described (23). Chimeric males were mated to C57BL/6J females, and resulting agouti progeny were tested for the presence of the mutation. Heterozygotes were mated to the Cre "deleter" mouse (25), and progeny were screened for removal of the neomycin gene by Cre-mediated site-specific recombination by using Southern transfer analyses as described in Figs. 1 and 2.

Fluorescence Imaging. Embryos derived from heterozygous intercrosses or crosses between heterozygous males and C57BL/6J females were harvested at gestational ages ranging from embryonic day (E) 7–9 for the *Hoxa1*^{GFPneo} allele. *Hoxc13*^{GFPneo} embryos were collected at E 11.5–17.5. Embryos were harvested, maintained, and imaged in Leibovitz's L-15 media lacking phenol red (GIBCO/BRL).

Embryos or tissue samples were either pinned to Sylgard (Dow Corning) plates or placed in glass depression slides under coverslips before imaging. GFP fluorescence was recorded using a Bio-Rad MRC 1024 Laser Scanning Confocal Imaging System fitted to a Leitz Aristoplan microscope. Standard fluorescein isothiocyanate activation wavelengths were used for the excitation of the GFP fluorochrome with a digital Kalman averaging filter to reduce random noise.

RESULTS

Vector Construction and Generation of Mutant Mice. We constructed a general cassette for use in generating *GFP* fusion genes by homologous recombination. The cassette contains an optimized *GFP* gene (6) that lacks the initiating methionine codon. Any one of three enzymes (see *Materials and Methods*) can be used to isolate the *GFP* gene, starting with the second codon, as well as the MC1neo gene (21) flanked by *lox*P sites. The initiation methionine codon of *GFP* was removed so that GFP expression requires fusion with the target gene. The GFP initiation methionine is not needed for GFP activity in fusion gene constructs (26–28). We used this cassette to generate targeting vectors for both *Hoxa1* and *Hoxc13*. In brief, the *Hoxa1* allele was designed to generate a protein fusion in the correct reading frame for all previously described *Hoxa1* splice variants (refs. 29 and 30; see Fig. 1). The *Hoxc13* allele generates a protein fusion at the same position that was used for the previously described *lac*Z fusion allele (ref. 23; see Fig. 2).

Targeting vectors were electroporated into R1 ES cells (24), which were subjected to positive–negative selection as described (22). Homologous recombination between the targeting vector and the *Hoxa1* locus was assessed by Southern transfer analysis of *Eco*RV digested genomic DNA (Fig. 1). Ten of 143 independent cell lines demonstrated homologous recombination. Germline transmission was demonstrated in agouti offspring of chimeras by the same Southern transfer analysis (Fig. 1*B*). Finally, removal of the neomycin resistance gene by Cre-mediated site-specific recombination was confirmed by Southern transfer analysis (Fig. 1*C*).

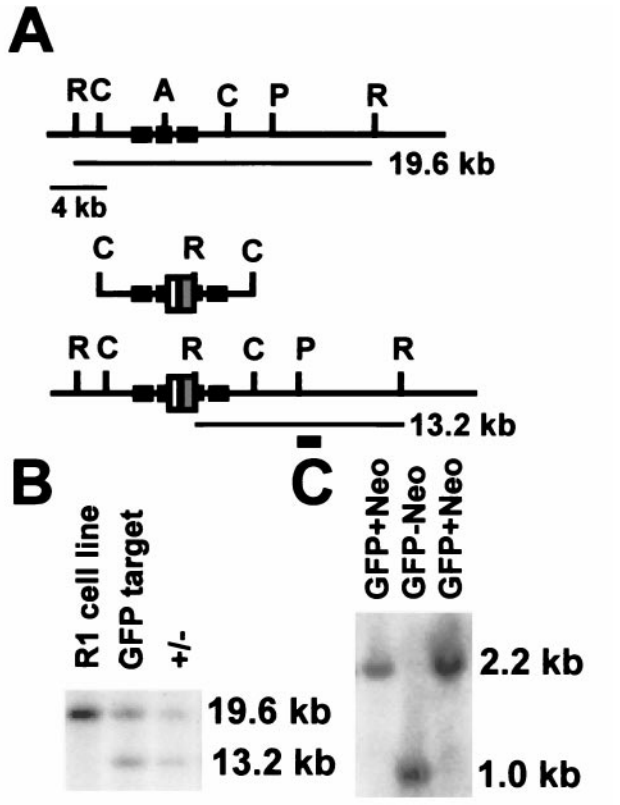

FIG. 1. Hoxa1^{GFPneo}-targeting vector and Southern blot analysis. (*A*) Large solid boxes represent *Hoxa1* exons, white box the *GFP* gene, and gray box the *lox*P flanked MC1neo cassette, *Aat*II (A), *Cla*I (C), and *Pac*I (P), and *Eco*RV (R). The position of the 3′-flanking probe used for Southern transfer analysis is indicated by the small solid box. The first line shows the wild-type genomic structure, the second line the targeting vector, and the third line the genomic structure resulting from homologous recombination. (*B*) Southern blot analysis of targeted cell line and chimera progeny. Shown are *Eco*RV digests of the parental R1 cell line, a targeted ES cell line, and offspring from a chimera. The wild-type allele is detected by a 19.6-kb restriction fragment, whereas the mutant allele is detected by a 13.2-kb restriction fragment. (*C*) Analysis of progeny of a *Hoxa1*^{GFPneo} heterozygote crossed to a Cre deleter mouse. Shown are Southern transfer analyses of *Bam*HI-digested DNA probed with an *Nco*I–*Afl*II pEGFP fragment. A 2.2-kb fragment is detected in the *Hoxa1*^{GFPneo} mice that shifts to 1.0 kb upon Cre-mediated removal of the neomycin resistance gene.

Eleven of 144 independent cell lines surviving positive–negative selection (22) had undergone homologous recombination for the *Hoxc13*^{GFPneo} allele as assayed by Southern transfer analysis (Fig. 2*B*). The removal of the neomycin gene by Cre-mediated site-specific recombination is shown in Fig. 2*C*. The same *Bam*HI restriction fragments used to characterize the targeted ES cell line were diagnostic for genotyping progeny of heterozygous intercrosses (Fig. 2*D*).

Expression of the Hoxa1^{GFPneo} Allele. Fluorescence due to expression of the Hoxa1-GFP fusion protein was detectable as early as E 6.5 (data not shown). Some autofluorescence was visible in wild-type embryos in regions proximal to sites of *Hoxa1*^{GFPneo} expression. However, while the extraembryonic endoderm autofluoresced at E 7.0, it became undetectable by E 8.25 (Fig. 3*A–D*). By E 8.25, the expression of the *Hoxa1*^{GFPneo} fusion gene recapitulates the expression pattern of *Hoxa1*, labeling both the presumptive rhombomere 3/4 region of the developing hindbrain and the posterior regression of primitive streak into the caudal neural tube (Fig. 3*C*).

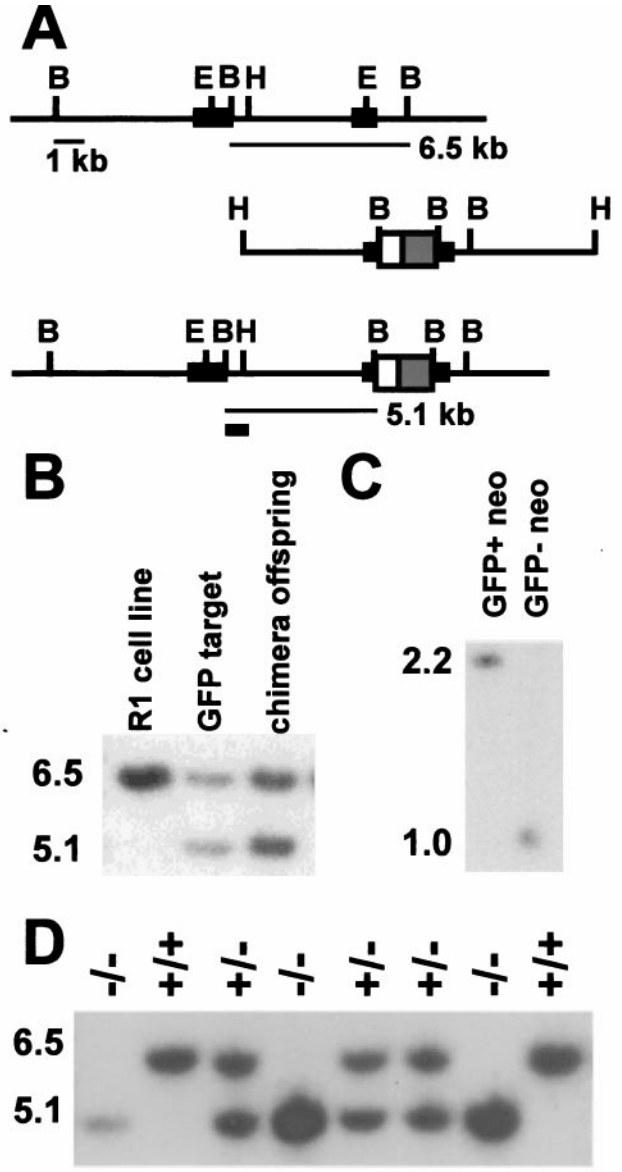

FIG. 2. Hoxc13^{GFPneo}-targeting vector and Southern blot analysis. (*A*) Genomic structure and targeting vector. Symbols in *A* are as described in Fig. 1, except large solid boxes represent *Hoxc13* exons, *Bam*HI (B), *Bst*EII (E), and *Hin*dIII (H). The position of the 5′-flanking probe used for Southern transfer analysis is indicated by the small solid box. (*B*) Southern blot analysis of targeted cell line and offspring from a chimera. Shown are *Bam*HI digests of the parental R1 cell line, a targeted ES cell line, and an offspring from a chimera. (*C*) Analysis of progeny of a *Hoxc13*^{GFPneo} heterozygote crossed to a Cre deleter mouse. Analysis is as described for Fig. 1*C*. (*D*) Genotypic analysis of a litter resulting from an intercross of *Hoxc13*^{GFPneo} allele heterozygotes. Southern transfer analysis of *Bam*HI-digested DNA was performed and shows two wild-type offspring carrying only the 6.5-kb fragment, three heterozygotes carrying both the 6.5- and 5.1-kb fragments, and three homozygous mutant offspring carrying only the 5.1-kb fragment.

Notably at E 8.75, GFP expression could no longer be detected in the hindbrain region of either heterozygous or homozygous embryos. This finding suggests that the *Hoxa1*^{GFPneo} fusion gene is regulated similarly to the normal *Hoxa1* gene, with no persistence of signal.

Concomitant with reduction of the signal in the hindbrain at E 8.75, expression becomes detectable in the epithelium of the foregut pocket (Fig. 3*E*). In this region, differentiation of the cardiogenic mesoderm, gut-associated mesoderm, and foregut endoderm appear to be mediated by inductive processes of the foregut endoderm and/or visceral yolk sac endoderm (31–33). *Hoxa1*^{GFPneo} expression also was detected in E 9.0 embryos in the most caudal regions of the neural tube and nephrogenic duct (Fig. 3*G–J*). GFP expression could not be detected in embryos older than E 9.5, confirming that the fusion gene again follows normal *Hoxa1* expression and regulation in early embryos. A splice variant of the *Hoxa1* gene expressed in adult intestine has been identified (34). Examination of adult intestines from wild-type and homozygous mutant mice revealed no GFP expression, although autofluorescence was seen in the intestinal vasculature in both wild-type and mutant samples. Initial experiments with *Hoxa1*^{GFPlox} embryos (lacking the neomycin resistance gene) show the same level and pattern of expression as shown in Fig. 3*C*.

Expression of Hoxc13^{GFPneo} and Hoxc13^{GFPlox} Alleles. Embryos were examined for expression in all spatial and temporal domains in which *Hoxc13* expression was previously detected (23). At E 11.5 fluorescence in the tail was evident in the somites and the neural tube (Fig. 4*A*). By E 13.5, fluorescence in the tail was restricted to the outer layers of the tail and to a subregion of the somites (Fig. 4 *B–D*). The same laser intensity and detection conditions were used for the various genotypes and clearly show lack of significant background autofluorescence in the wild-type tail (Fig. 4*B*) and reduced fluorescence in the heterozygote (one *Hoxc13*^{GFPneo} allele; Fig. 4*C*) as compared with the homozygote (two *Hoxc13*^{GFPneo} alleles; Fig. 4*D*). Higher magnifications of E 13.5 tails showed expression in a sub-domain of the somites adjacent to the midline (Fig. 4*E*). In addition, the highest magnification of the tail (Fig. 4*F*) reveals that GFP expression can be resolved in single cells. The same pattern of expression in the tail was also detected using a *Hoxc13*^{GFPlox} heterozygote (i.e., after removal of the neomycin gene; cf. Fig. 4 *C* and *G*). GFP expression also is seen in the nails and vibrissae at E 13.5 in a *Hoxc13*^{GFPlox} heterozygote (Fig. 4*H*). At E 15.5 (Fig. 4 *I–J*), strong GFP expression fills much of the nail, although differences in signal width are already detectable depending on the focal plane of the laser. In addition, while 5-bromo-4-chloro-3-indolyl β-D-galactoside (X-gal) staining of E 17.5, *Hoxc13*^{lacZneo} embryos revealed an interesting talon-shaped expression pattern in the nails (23), optical sectioning of GFP embryos revealed that this area of Hoxc13 expression is restricted to a very thin cell layer. This cell layer is horizontal at the base of the nail and curves around the sides of the nail ventrally forming a curved planar sheet (data not shown). Furthermore, the restricted expression in the somites at E 13.5 (Fig. 4*E*) was masked by β-galactosidase (β-gal) staining in the outer layers of the tail (23). Thus, Hoxc13-GFP expression was detected in all domains previously described (23) including tail, nails, and vibrissae (see Fig. 4) as well as in the hair follicles and the filiform papillae of the tongue (data not shown). However, much higher resolution of the spatial aspects of *Hoxc13* nail and tail expression was possible with the *GFP* allele.

Hoxc13^{GFPlox} homozygotes (i.e., from which the neomycin gene has been removed from both mutant alleles by CRE recombinase) are phenotypically indistinguishable from *Hoxc13*^{GFPneo} homozygotes, as well as from the previously described *Hoxc13*^{neo} and *Hoxc13*^{lacZneo} homozygotes (Fig. 5*A*; ref. 23). This observation argues that all of the previously described mutant defects (23) in the formation of hair, nails, and filiform papillae are due to the absence of the Hoxc13 protein, rather than to interfering effects of the neomycin cassette on the transcription of neighboring genes. Interestingly, in contrast to *Hoxc13*^{neo} or *Hoxc13*^{lacZneo} heterozygotes (23), both *Hoxc13*^{GFPneo} (Fig. 5*C*) and *Hoxc13*^{GFPlox} (data not shown) heterozygotes have abnormal hair phenotypes. Notably, while the dorsal coat appears relatively normal, the ventral coat is sparse, especially in females. This suggests that some breakage of hair occurs in heterozygotes (Fig. 5*C*). In addition, at some stages of the hair cycle, lower portions of the face,

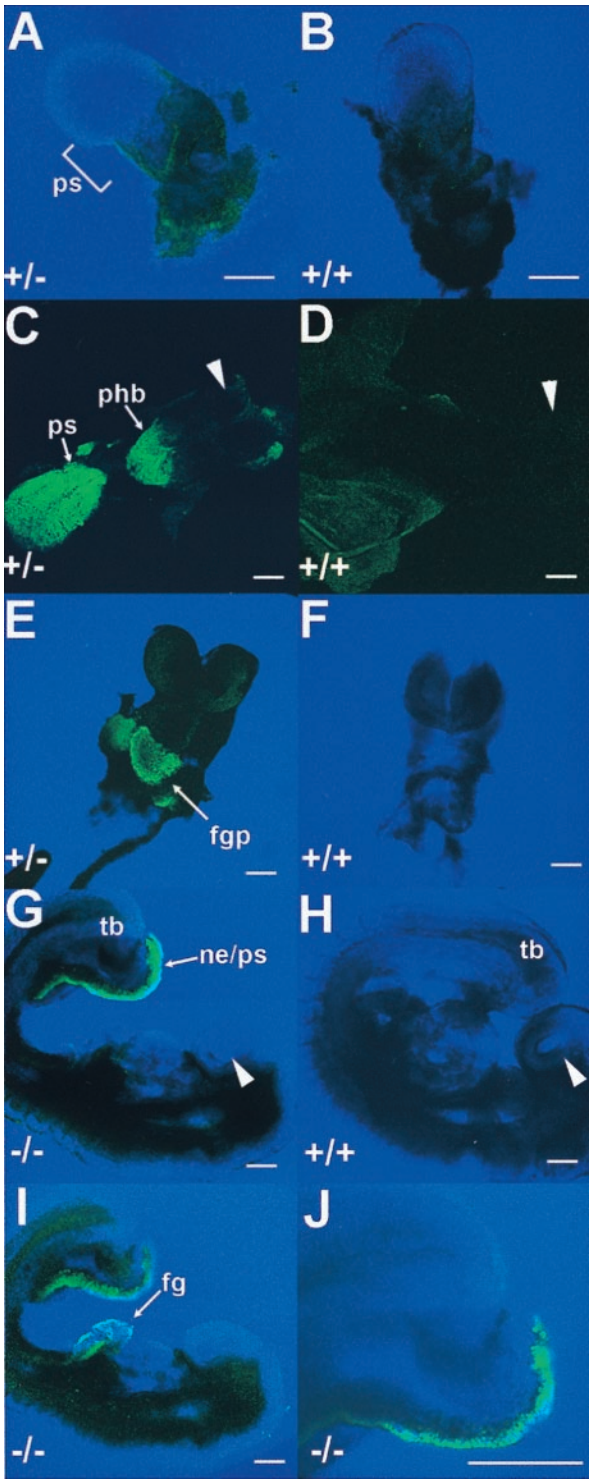

FIG. 3. Embryonic expression of the *Hoxa1*^{GFPneo} allele. (*A*) Expression in *Hoxa1*^{GFPneo} heterozygote at E 7.0 in the primitive streak (ps). (*B*) Autofluorescence of extra-embryonic tissues in a wild-type embryo at E 7.0. Note same level of autofluorescence in a heterozygote (A). (*C*) Expression at E 8.25 in *Hoxa1*^{GFPneo} heterozygote in rhombomere 3/4 of the presumptive hindbrain (phb), the regressing primitive streak (ps), and tail bud. Arrowhead indicates dorsal headfold region. (*D*) Lack of autofluorescence in a wild-type embryo at E 8.25 by using the same microscopic conditions as in *C*. Arrowhead indicates dorsal headfold region. (*E*) Expression in the developing foregut pocket (fgp) at E 8.75 in a *Hoxa1*^{GFPneo} heterozygote. (*F*) Lack of fluorescence in a wild-type embryo at E 8.75 by using the same microscopic conditions as in *E*. (*G*) Expression in a *Hoxa1*^{GFPneo} homozygote at E 9.0 in the caudal most region of the embryo in the nephrogenic duct (ne), tail bud (tb), and primitive streak (ps). Arrowhead indicates nasal placode. (*H*) Lack of fluorescence in wild-type embryo at E 9.0 by using the same microscopic conditions as in *G* and *I*. Arrowhead indicates nasal placode. (*I*) Expression in a *Hoxa1*^{GFPneo} homozygote at E 9.0 in the foregut (fg) and tail bud (tb). (*J*) Higher magnification image of caudal expression showing single cell resolution. (For *A–J*, scale bar is 20 microns.)

especially below and behind the eyes, show patchy fur (Fig. 5*D*).

It is possible that the phenotypic difference between the *Hoxc13*^{GFP} and the *Hoxc13*^{lacZneo} heterozygotes reflects the ability of the fusion proteins to interact with other proteins or the transcription complex. The large size of the β-gal fusion protein in either monomeric or tetrameric form may be sufficient to block a specific protein–protein interaction, while the smaller Hoxc13-GFP monomer can still interact leading to the observed hair phenotype in heterozygotes. An earlier study using a fibroblast growth factor receptor 1–β-gal fusion found transformation of cells due to receptor activation by β-gal tetramerization, while using fusion genes from which the tetramerization domain was removed did not transform cells (5). This example demonstrates that β-gal fusion protein tetramerization does have the potential to affect fusion protein function.

DISCUSSION

The use of targeted *GFP* fusion genes to track gene expression in living cells should enhance several avenues of research in murine development in general and *Hox* gene research in particular. For example, vital marking of cells containing targeted disruptions of specific genes will facilitate the analysis of cell autonomy of specific phenotypes, the analysis of cell migration, and examination of the contribution of cells expressing a given gene to the region affected by a mutation. In addition, since Leibovitz's media appears to maintain embryo viability for at least 3 hr, analysis of gene expression in the same embryo at several time points may be feasible without special culture chambers. We have observed in early embryos (E 8–8.5) that sustained confocal laser imaging does exert some damage to embryonic tissues. Recently, we have found that combining digital imaging with the GFP 500/470 nm filter cube set available for the MZ12 dissecting microscope (Leica) or the SMZU stereo-microscope (Nikon) allows analysis of our single copy gene fusions without damage. Indeed, single copy *Hoxc13*^{GFPneo} or *Hoxc13*^{GFPlox} fusion gene expression is detectable in embryos even without the use of digital capture technology. However, the signal strength is greatly augmented with digital capture, e.g., using a 3CCD camera (Dage–MTI, Michigan City, IN). Finally, preliminary comparisons of GFPneo and GFPlox alleles for both *Hoxa1* and *Hoxc13* revealed that removal of the neomycin gene and its promoter/enhancer did not affect either the level or pattern of expression.

The *Hoxa1* locus encodes two alternatively spliced mRNAs, which appear to be differentially expressed in the developing mouse embryo (34). From E 7–8.5, both transcripts are expressed equally within the neural tube in the presumptive rhombomere 3/4 region of the hindbrain. However, later in development (E 9.5) and continuing in the adult, only the non-homeodomain encoding mRNA is expressed within the developing foregut region and adult intestine. Aside from a uniform reduction in signal in heterozygotes, no temporal or spatial differences in *Hoxa1*^{GFPneo} expression were detected between heterozygous and homozygous embryos. This finding suggests that the *Hoxa1* gene product(s) are not required for maintenance of *Hoxa1* expression.

The expression of the *Hoxa1* fusion gene in the epithelium of the foregut pocket may provide a means to investigate

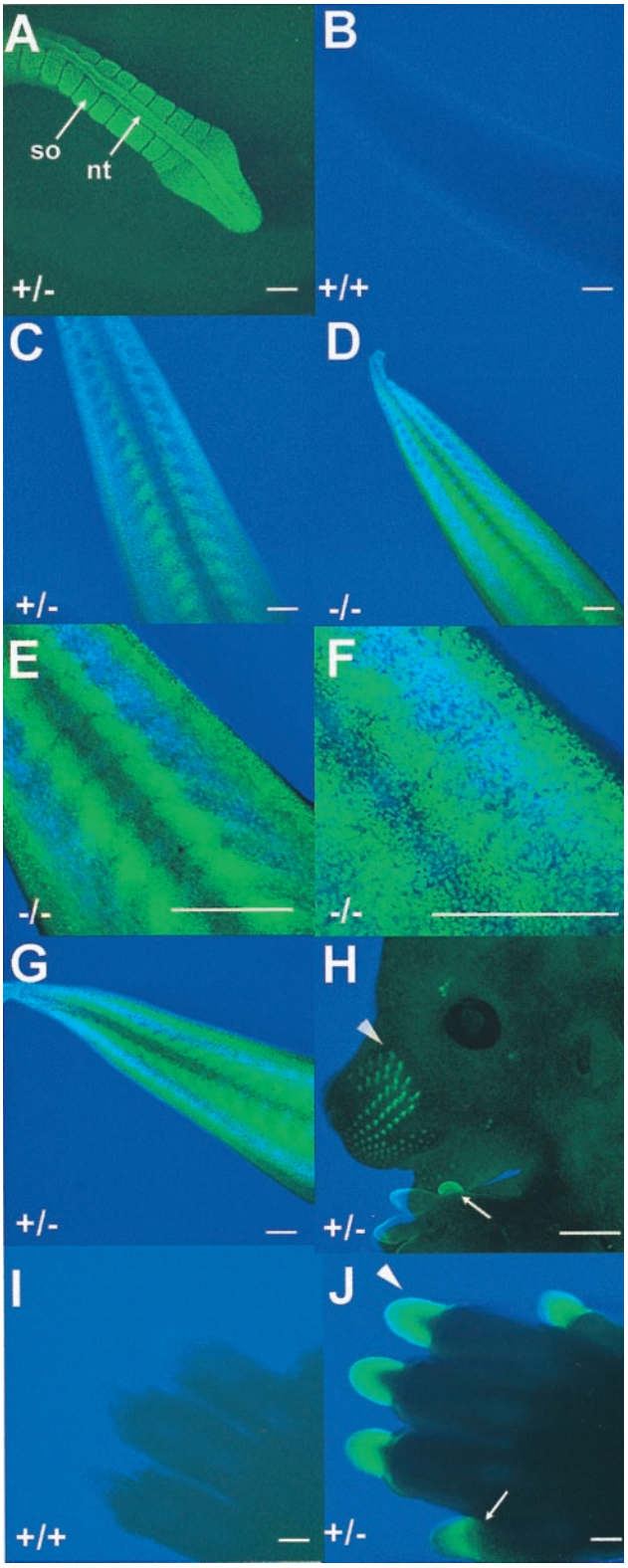

FIG. 4. Expression of the *Hoxc13*^{GFPneo} and *Hoxc13*^{GFPlox} alleles. (*A*) Neural tube (nt) and somite (so) expression in the tail of a *Hoxc13*^{GFPneo} heterozygote at E 11.5. (*B*) Tail expression in a wild-type embryo at E 13.5. The same microscopic conditions were used for *B-D*. (*C*) Tail expression in a *Hoxc13*^{GFPneo} heterozygote at E 13.5. (*D*) Tail expression in a *Hoxc13*^{GFPneo} homozygote at E 13.5. (*E*) Higher magnification of tail expression in *Hoxc13*^{GFPneo} homozygote at E 13.5. (*F*) Higher magnification of tail expression in a *Hoxc13*^{GFPneo} homozygote at E 13.5. (*G*) Tail expression in *Hoxc13*^{GFPlox} heterozygote at E 13.5. (*H*) Vibrissae (arrowhead) and nail (arrow) expression in a *Hoxc13*^{GFPlox} heterozygote at E 13.5. (*I*) Nail expression in a wild-type embryo at E 15.5. (*J*) Nail expression in a *Hoxc13*^{GFPneo} heterozygote at E 15.5. The same microscopic conditions were used for *I* and *J*. Wild-type embryos showed no fluorescence under the same experimental conditions used for *A*, *G*, and *H* (data not shown). (Scale bar is 20 microns, except for *H* where it is 500 microns).

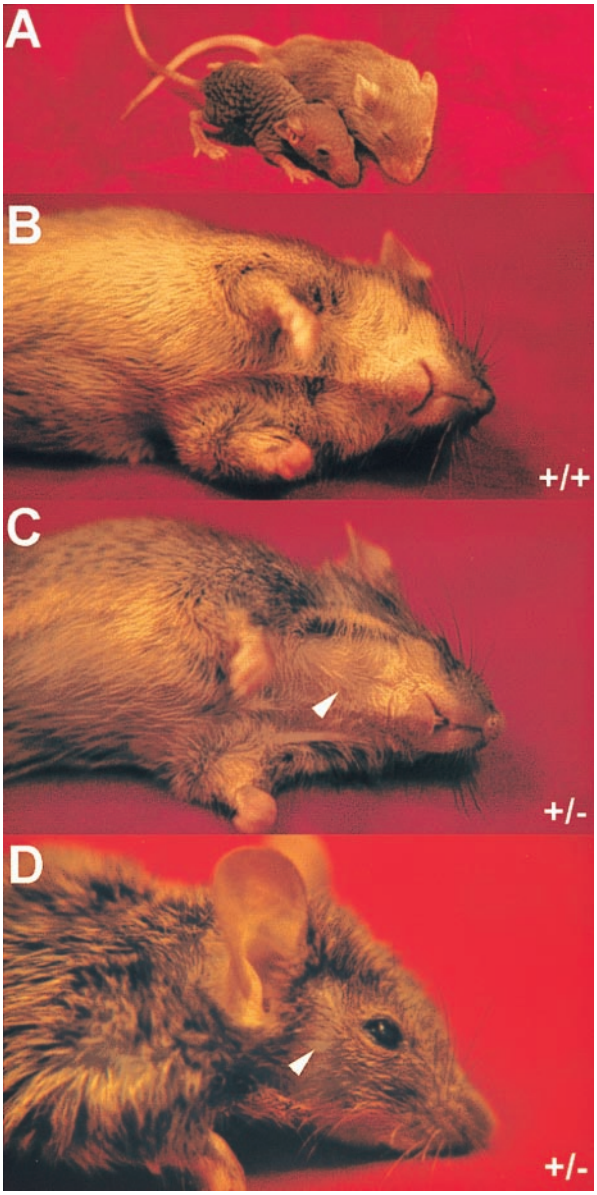

FIG. 5. Hair phenotype of *Hoxc13*^{GFPneo} and *Hoxc13*^{GFPlox} mice. (*A*) Wild-type and *Hoxc13*^{GFPlox} homozygous littermates at postnatal day 16. (*B*) Wild-type mouse ventral side. (*C*) *Hoxc13*^{GFPneo} heterozygous littermate ventral side. Arrowhead indicates a region of fur that is patchy. (*D*) *Hoxc13*^{GFPneo} heterozygous face. Arrowhead indicates a region of fur that is patchy.

inductive interactions between the endodermally derived gut epithelium and mesodermally derived cardiomyocytes. Of particular interest is the immediate proximity of the *Hoxa1*^{GFPneo}-expressing cells and the cardiomyocytes within the foregut pocket. It is important to note that no cardiac malformations have been reported in mice with a targeted disruption of *Hoxa1*. However, given the role *Hoxa1* has in patterning the hindbrain and lateral mesoderm, it is conceivable that this gene also might have either direct or indirect roles in patterning the foregut pocket and subsequent cardiac region. The fusion gene functions well as a vital marker early

in hindbrain and foregut development. In particular, distinct tissue layers as well as individual cells expressing this vital marker are readily identifiable laying the foundation for future studies addressing cell autonomy within *Hoxa1* mutants.

Because the *Hoxc13*^{lacZneo} (23) and *Hoxc13*^{GFPneo} fusion gene alleles disrupt the *Hoxc13*-coding region at exactly the same position, the two marker systems can be objectively compared. Both markers generate identical expression patterns that match RNA whole mount *in situ* analysis for *Hoxc13* from E 9.5 to E 14.5 (23). Unexpectedly, the *lac*Z and *GFP* mutant alleles behave differently in heterozygous mice. This result illustrated that the marker gene itself can influence the behavior of the fusion gene allele by affecting parameters, such as accessibility to cellular components or mRNA and fusion protein stability. One major advantage of the *GFP* allele is the ability to reconstruct the detailed three-dimensional aspects of the expression patterns by using the optical sectioning capabilities of laser-based confocal systems, precluding the necessity to section or hemisect and clear β-gal-stained embryos. The *Hoxc13*^{GFPlox} allele should prove useful not only for examining dynamic expression changes over time but also for isolating specific cell types expressing *Hoxc13* for more detailed analysis.

In conclusion, use of targeted *GFP* fusion genes should add to the repertoire of techniques available for studies of gene expression and gene function. We have shown that expression from single-copy *GFP*-targeted alleles is detectable both early and late in embryogenesis. The ability to analyze the change in expression pattern over time in the same individual as well as the potential ability to use fluorescence-activated cell sorting to isolate pure populations of cells expressing a gene of interest fused to *GFP* should greatly aid understanding of *Hox* function.

We thank M. Allen, S. Barnett, J. Hayes, C. Lenz, G. Peterson, and M. Wagstaff for expert technical assistance, members of the Capecchi lab for critical reading of the manuscript and advice, and L. Oswald for help with preparation of the manuscript. A.R.G. and H.S.S. were associates of the Howard Hughes Medical Institute. A.R.G. also was supported, in part, by the G. Harold and Leila Y. Mathers Charitable Foundation.

1. Chalfie, M., Tu, Y., Euskirchen, G., Ward, W. W. & Prasher, D. C. (1994) *Science* **263,** 802–805.
2. Heim, R., Prasher, D. C. & Tsien, R. Y. (1994) *Proc. Natl. Acad. Sci. USA* **91,** 12501–12504.
3. Prasher, D. C. (1995) *Trends Genet.* **11,** 320–323.
4. Jacobson, R. H., Zhang, X.-J., DuBose, R. F. & Matthews, B. W. (1994) *Nature (London)* **369,** 761–766.
5. Kouhara, H., Kurebayashi, S., Hashimoto, K., Kasayama, S., Koga, M., Kishimoto, T. & Sato, B. (1995) *Oncogene* **10,** 2315–2322.
6. Yang, T.-T., Cheng, L. & Kain, S. R. (1996) *Nucleic Acids Res.* **24,** 4592–4593.
7. Cormack, B. P., Valdivia, R. H. & Falkow, S. (1996) *Gene* **173,** 33–38.
8. Okabe, M., Ikawa, M., Kominami, K., Nakanishi, T. & Nishimune, Y. (1997) *FEBS Lett.* **407,** 313–319.
9. Ikawa, M., Kominami, K., Yoshimura, Y., Tanaka, K., Nishimune, Y. & Okabe, M. (1995) *Dev. Growth Differ.* **37,** 455–459.
10. Zhou, L., Sun, B., Zhang, C.-L., Fine, A., Chiu, S.-Y. & Messing, A. (1997) *Dev. Biol.* **187,** 36–42.
11. Amsterdam, A., Lin, S., Moss, L. G. & Hopkins, N. (1996) *Gene* **173,** 99–103.
12. Amesterdam, A., Lin, S. & Hopkins, N. (1995) *Dev. Biol.* **171,** 123–129.
13. Higashijima, S.-I., Okamoto, H., Ueno, N., Hotta, Y. & Eguchi, G. (1997) *Dev. Biol.* **192,** 289–299.
14. Long, Q., Meng, A., Wang, H., Jessen, J. R., Farrell, M. J. & Lin, S. (1997) *Development (Cambridge, U.K.)* **124,** 4105–4111.
15. Meng, A., Tang, H., Ong, B. A., Farrell, M. J. & Lin, S. (1997) *Proc. Natl. Acad. Sci. USA* **94,** 6267–6272.
16. Zernicka-Goetz, M., Pines, J., Ryan, K., Siemering, K. R., Haseloff, J., Evans, M. J. & Gurdon, J. B. (1996) *Development (Cambridge, U.K.)* **122,** 3719–3724.
17. Zernicka-Goetz, M., Pines, J., McLean Hunter, S., Dixon, J. P. C., Siemering, K. R., Haseloff, J. & Evans, M. J. (1997) *Development (Cambridge, U.K.)* **124,** 1133–1137.
18. Deng, C., Bedford, M., Li, C., Xu, X., Yang, X., Dunmore, J. & Leder, P. (1997) *Dev. Biol.* **185,** 42–54.
19. Friedrich, G. & Soriano, P. (1991) *Genes Dev.* **5,** 1213–1223.
20. Mansour, S. L., Thomas, K. R., Deng, C. & Capecchi, M. R. (1990) *Proc. Natl. Acad. Sci. USA* **87,** 7688–7692.
21. Thomas, K. R. & Capecchi, M. R. (1987) *Cell* **51,** 503–512.
22. Mansour, S. L., Thomas, K. R. & Capecchi, M. R. (1988) *Nature (London)* **336,** 348–352.
23. Godwin, A. R. & Capecchi, M. R. (1998) *Genes Dev.* **12,** 11–20.
24. Nagy, A., Rossant, J., Nagy, R., Abramow-Newerly, W. & Roder, J. C. (1993) *Proc. Natl. Acad. Sci. USA* **90,** 8424–8428.
25. Schwenk, F., Baron, U. & Rajewsky, K. (1995) *Nucleic Acids Res.* **23,** 5080–5081.
26. Marshall, J., Molloy, R., Moss, G. W. J., Howe, J. R. & Hughes, T. E. (1995) *Neuron* **14,** 211–215.
27. Li, X., Zhang, G., Ngo, N., Zhao, X., Kain, S. R. & Huang, C.-C. (1997) *J. Biol. Chem.* **272,** 28545–28549.
28. Dopf, J. & Horiagon, T. M. (1996) *Gene* **173,** 39–44.
29. Baron, A., Featherstone, M. S., Hill, R. E., Hall, A., Galliot, B. & Duboule, D. (1987) *EMBO J.* **6,** 2977–2986.
30. LaRosa, G. J. & Gudas, L. J. (1988) *Mol. Cell. Biol.* **8,** 3906–3917.
31. Jacobson, A. G. & Sater, A. K. (1988) *Development (Cambridge, U.K.)* **104,** 341–359.
32. Stöhr, P. H. (1924) *Wilhelm Roux' Arch. Entwicklungsmech. Org.* **102,** 426–451.
33. Narita, N., Bielinska, M. & Wilson, D. B. (1997) *Dev. Biol.* **189,** 270–274.
34. Murphy, P. & Hill, R. E. (1991) *Development (Cambridge, U.K.)* **111,** 61–74.